Electronic Supplementary Information for

High-Purity Iron Pyrite (FeS_2) Nanowires as High-Capacity Nanostructured Cathodes for Lithium-Ion Batteries

Linsen Li[¶], Miguel Cabán-Acevedo[¶], Steven N. Girard, and Song Jin*
Department of Chemistry, University of Wisconsin-Madison, 1101 University Avenue, Madison, Wisconsin 53706, United States

[¶] These authors contributed equally to this work.

*E-mail: jin@chem.wisc.edu

EXPERIMENTAL METHODS

Materials. All chemicals were used as received without further purification. Hydrofluoric acid (aqueous HF solution, 48 wt%, CAS # 7664-39-3. *Warning: HF solution is highly corrosive and must be handled with care and proper protection. Please see safety information*[S1]), iron (III) nitrate nonahydrate [$Fe(NO_3)_3{\cdot}9H_2O$, ≥98.0%, CAS # 7782-61-8], elemental sulfur (S, 99.5–100.5%, CAS # 7704-34-9), lithium bis(trifluoromethane)sulfonimide (LiTFSi, 99.95% trace metal basis, CAS # 90076-65-6), and tetraethylene glycol dimethyl ether (TEGDME, ≥99.0%, CAS # 143-24-8) were purchased from Sigma Aldrich. Ethanol (200 proof, CAS # 64-17-5) was purchased from Decon Laboratories Inc. N-methyl-2-pyrrolidone (NMP, ≥99.5%, CAS # 872-50-4), polyethylene separator membranes, polyvinylidene difluoride (PVDF, ≥99.5%, CAS # 24937-79-9) binder, lithium foils (15.6 mm in diameter × 0.45 mm in thickness, >99%, CAS # 7439-93-2) and 2032-type coin cell cases were purchased from MTI Corporation. Carbon black [Super P® conductive, ≥99% (metal basis), CAS # 1333-86-4] and aluminum foils [0.025 mm in thickness, ≥99.45% metal basis, CAS # 7429-90-5] were purchased from Alfa Aesar.

Nanowire Synthesis. The α-$FeF_3{\cdot}3H_2O$ nanowires (NWs) were prepared *via* an improved synthesis based on our previous work.[S2] Briefly, 7.5 mL ethanol and 2.0 mL HF aqueous solution (48 wt%) were carefully added into a 15 mL plastic centrifuge tube in sequence. The centrifuge tube was sealed and gently shaken by hand with great caution to allow the two liquids to mix. An Fe^{3+} solution in ethanol with a concentration of 266 mM was made by dissolving 1.616 g $Fe(NO_3)_3{\cdot}9H_2O$ in 15.0 mL ethanol. 0.500 mL of this Fe^{3+}/ethanol solution was then quickly injected into the HF/ethanol mixture using an Eppendorf pipet. The resulting colorless solution with a concentration ratio of $c(Fe^{3+})$: c(HF) : $c(H_2O)$ ≈ 13.3 mM: 5560 mM: 6760 mM was gently mixed by shaking and kept in an oven at 60 °C for 24 h. No substrate was used during the reaction and aggressive agitation was avoided to suppress the formation of large β-$FeF_3{\cdot}3H_2O$ crystals. The white cloudy precipitate that appeared over time was collected by centrifugation at 5000 rpm for 5 min, washed with dry ethanol twice and vacuum-dried at room temperature. Typically, 6.6–7.7 mg NWs can be acquired from a 10 mL-scale reaction, corresponding to a yield of 30–35% based on the limiting agent of Fe.

The $FeF_3{\cdot}3H_2O$ NWs (~10 mg) were transferred to an alumina boat, which was loaded at the center of a home-made flow tube reactor setup with flow and pressure control. The $FeF_3{\cdot}3H_2O$ NWs were first dehydrated under vacuum by slowly heating to a 100 °C at a rate of ~2 °C/min, then to 200 °C at a rate of ~ 0.5 °C min^{-1}. The powder color changed from white to green/brown.

Then the sulfidation reaction was carried out at 500 °C for 2 h under a sulfur atmosphere. An alumina boat containing ~3 g elemental sulfur was introduced and positioned at a temperature of ~415 °C throughout the reaction, which yields an estimated sulfur vapor pressure of ~480 Torr.[S3] After 2 h of reaction the reactor was evacuated and the tube furnace was open to allow the reactor to cool down naturally to room temperature. Larger scale of conversion (~80 mg) could also be readily carried out in a closed ampule using sufficient amount of sulfur to ensure a saturated sulfur atmosphere at 500 °C.

Material Characterization. Scanning electron microscopy (SEM) images were acquired using a LEO 55 VP field emission scanning electron microscope at a working voltage of 2 kV. Transmission electron microscopy (TEM) images and electron diffraction (ED) patterns were acquired using a Philips CM200 transmission electron microscope at an accelerating voltage of 200 kV. The TEM samples were prepared by dropcasting FeS_2 NWs suspended in ethanol onto lacey-carbon grids (Ted Pella Inc. lacey carbon type-A, 300 Mesh). All the TEM grids were checked for appropriate NW density using an optical microscope before TEM characterization. High-resolution X-ray diffraction was performed by synchrotron radiation at Argonne National Laboratory on the Advanced Photon Source (APS), beamline 11-BM using a 12-analyzer Si detector and calibrated radiation wavelength of 0.412455 Å.[S4, S5] The samples were hand ground using a mortar and pestle and passed through a 40 μm steel mesh sieve. The resulting fine powders were packed into 0.5 mm quartz capillaries and evacuated to a residual vacuum of ~10^{-3} Torr and flame-sealed using a high temperature torch. The capillaries were placed in a double-tilt goniometer in transmission geometry (Debye-Scherrer method) and rotated at 500 rpm. The confocal micro-Raman spectra of an as-synthesized sample on borosilicate substrate were collected with a Horiba Jobin Yvan LabRAM ARAMIS confocal microscope using a 100 μm aperture and a 532 nm laser source. Optical measurements were performed using a Cary-5000 UV-Vis-NIR spectrophotometer equipped with an integration sphere (Agilent Technologies).

Nano-pyrite Cathode Processing and Electrochemical Measurements. Electrochemical measurements were performed on nanocomposite electrodes pasted on aluminum foils, which were prepared from slurries containing 70 wt% FeS_2 NWs, 20 wt% conductive carbon black, and 10 wt% PVDF binder using NMP as the solvent. The mass loading of active material (FeS_2) was about 2–3 mg cm^{-2}. CR2032-type coin cells were assembled in an argon-fill glovebox, using Li metal as the counter/quasi-reference electrode, 1 M LiTFSi in TEGDME as the electrolyte, polyethylene films as the separator. All cells were aged overnight before electrochemical tests. Discharge/charge cycling tests were performed with a multi-channel battery analyzer (MTI BST8-WA) operated using Neware software at room temperature (~25 °C) over different voltage windows at different current densities from 0.01 C to 0.2 C (1 C = 894 mA g^{-1}). All reported performance was calculated based on the mass of the active material (FeS_2). Electrochemical impedance spectroscopy (EIS) were performed using a Biologic SP-200 Potentiostat operated using EC-Lab software over a frequency range from 200 kHz to 50 mHz with a perturbation voltage of 10 mV. The cells were rest for 0.5 h before taking the EIS measurements. Cyclic voltammogram was measured using a Biologic SP-200 Potentiostat operated using EC-Lab software. The cell was cycled between 2.4 V and 0.7 V vs Li^+/Li at a scan rate of 0.2 mV·s^{-1}.

ADDITIONAL TABLES AND FIGURES

Table S1. List of the free energy of formation ($\Delta_f G$, in kJ mol^{-1}) for FeS_2 and SF_6.

Chemical Species	Free Energy of Formation ($\Delta_f G$) / kJ mol^{-1}				
	600 K	700 K	**773 K**	800 K	900 K
FeS_2 (*s*)	–143.86	–137.074	**–131.035**	–129.946	–120.367
SF_6 (*g*)	–1008.204	–971.804	**–944.911**	–935.416	–897.998

Notes:

1) Values for 600 K, 700 K, 800 K, and 900 K are taken from the NIST-JANAF Thermochemical Tables (http://kinetics.nist.gov/janaf/). The values for 773 K were linearly extrapolated from the tabulated values.

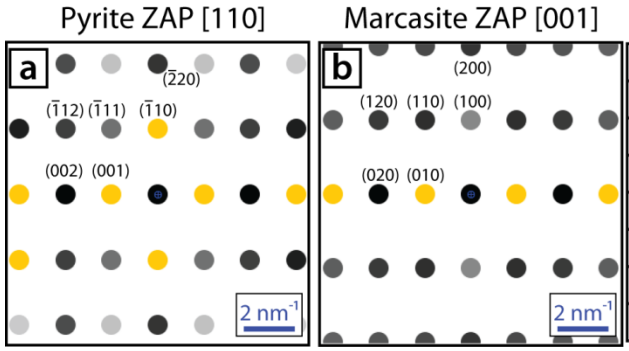

Pyrite [110]		Marcasite [001]	
(hkl)	d^{-1} / nm^{-1}	(hkl)	d^{-1}/ nm^{-1}
(001)	1.84	(010)	1.84
(002)	3.69	(020)	3.69
(1̄10)	2.61	(100)	2.25
(1̄11)	3.20	(110)	2.91
(1̄12)	4.52	(120)	4.32
(2̄20)	5.22	(200)	4.50

Figure S1. Simulated ZAPs for the pyrite [110] (a) in comparison with the ZAP for the marcasite [001] (b). Tables of the respective lattice spacings for the individual zone axis patterns are provided for numerical comparison. Double diffraction spots are included. The scalar bars in (a) and (b) have the same length and both correspond to 2 nm^{-1}. Simulated pattern are generated using JEMS electron microscopy software.

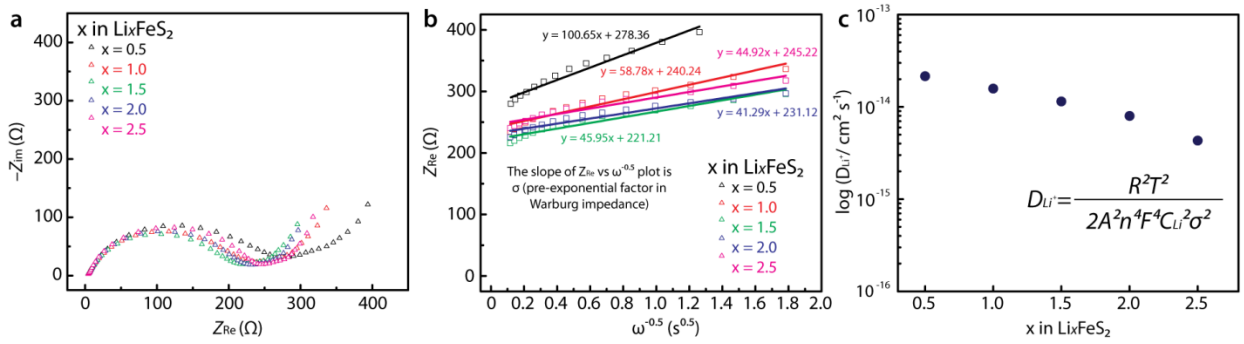

Figure S2. (a) EIS spectra ($-Z_{im}$ vs. Z_{Re} plot) measured at different states of lithiation. The measurements were done on the same coin cell in the frequency range from 200 kHz to 50 mHz with a perturbation voltage of 10 mV. The battery cell was discharged at 0.1 C rate (89.4 mA g^{-1}) to certain states of lithiation and allowed to rest 0.5 h before each EIS measurement; (b) Z_{Re} vs $\omega^{-1/2}$ plots at different states of lithiation (only the data in diffusion-controlled regime were plotted, where f = 11.7–0.05 Hz.) ω is the radial frequency. Note that the slope of the Z_{Re} vs $\omega^{-1/2}$ plot is σ (pre-exponential factor in Warburg impedance);[S6, S7] (c) Chemical diffusion coefficient D_{Li} at different states of lithiation. D_{Li} is calculated using the equation $D_{Li} = \frac{R^2T^2}{2A^2n^4F^4C_{Li}^2\sigma^2}$,[S6, S7]

where R is the gas constant (8.314 J K^{-1} mol^{-1}), T is the temperature (298.15 K), A is the surface area of the electrode (1.27 cm^2), n is the charge carried by Li^+ (n = 1), F is the Faraday constant (96485 C mol^{-1}), σ is the pre-exponential factor in Warburg impedance obtained from the slope of Z_{Re} vs $\omega^{-1/2}$ plot, and C_{Li} is the concentration of Li^+ in the solids (mol cm^{-3}). We used the volume of Li_2FeS_2 (intermediate phase during lithiation of FeS_2) crystal lattice to estimate C_{Li}.

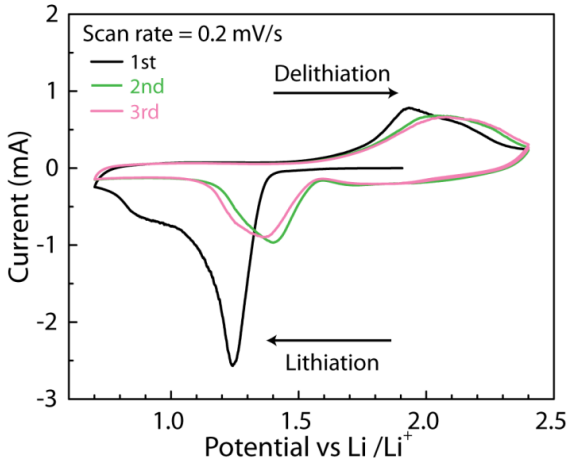

Figure S3. Cyclic voltammogram of a nano-pyrite cathode cycled between 2.4 V and 0.7 V vs Li^+/Li at a scan rate of 0.2 $mV{\cdot}s^{-1}$. The first three cycles are shown. This result agrees with our discussion on the electrochemistry section and previous reports[S8, S9] In the first lithiation cycle, two reactions ($FeS_2 + 2Li^+ + 2e^- \rightarrow Li_2FeS_2$ and $Li_2FeS_2 + 2Li^+ + 2e^- \rightarrow 2Li_2S + Fe^0$) proceed simultaneously due to the slow diffusion of Li^+ into pyrite at ambient temperature, which gives rise to a lithiation peak at ~1.25 V. In the first delithiation cycle, only $Li_{2-x}FeS_2$ ($0 < x < 0.8$) was formed and pyrite was not recovered when recharged to 2.4 V, as the delithiation peak area is clearly smaller than the first lithiation peak area. In subsequent two cycles, the cycling appeared to be quite reversible [$Li_{2-x}FeS_2 + (2+x)Li^+ + (2+x)\ e^- \rightleftarrows Fe^0 + 2Li_2S$ ($0 < x < 0.8$)], as the lithiation and delithiation peak areas were almost the same. It is also important to notice that no other redox peaks were observed in subsequent cycling, which ruled out other electrochemical processes (such as cycling of a pure Li_2S cathode or a sulfur cathode).

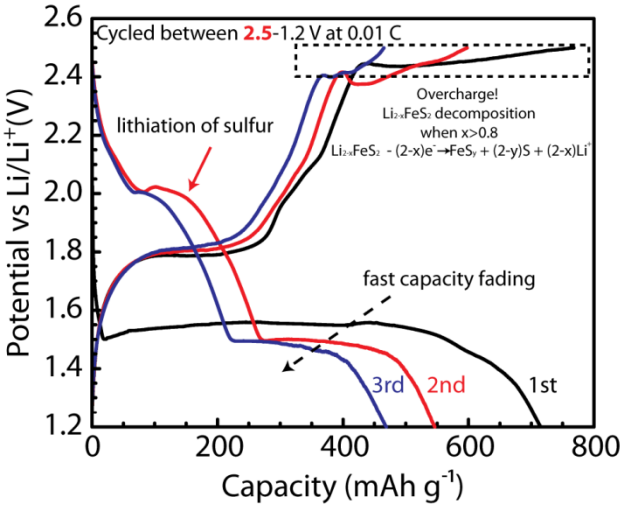

Figure S4. Voltage profile of a Li/nano-pyrite cell cycled in 2.5–1.1 V voltage range showing the voltage plateau originated from $Li_{2-x}FeS_2$ decomposition upon recharge beyond 2.4 V (highlighted in the dashed box in the upper right corner) and fast capacity fading in subsequent cycles.

References

[S1] Safety Information of Hydrofluoric Acid. http://www.sigmaaldrich.com/catalog/ProductDetail.do?lang=en&N4=30107|SIAL&N5=SEARCH_CONCAT_PNO|BRAND_KEY&F=SPEC

[S2] L. Li; Y. Yu; F. Meng; Y. Tan; R. J. Hamers; S. Jin. *Nano Lett.* **2012,** *12*, 724.

[S3] D.-Y. Peng; J. Zhao. *J. Chem. Thermodyn.* **2001,** *33*, 1121.

[S4] P. L. Lee, D. Shu, M. Ramanathan, C. Preissner, J. Wang, M. A. Beno, R. B. Von Dreele, L. Ribaud, C. Kurtz, S. M. Antao, X. Jiao, B. H. Toby, *J. Synchrotron Rad.* **2008,** 15, 427.

[S5] J. Wang, B. H. Toby, P. L. Lee, L. Ribaud, S. M. Antao, C. Kurtz, M. Ramanathan, R. B. V. Dreele, M. A. Beno, *Rev. Sci. Instrum.* **2008,** 79, 085105.

[S6] C. Ho, I. D. Raistrick and R. A. Huggins, *J. Electrochem. Soc.*, **1980,** 127, 8.

[S7] N. Takami; A. Satoh; M. Hara; T. Ohsaki. *J. Electrochem. Soc.* **1995,** *142*, 9.

[S8] R. Fong,J. R. Dahn, and C. H. W. Jones. *J. Electrochem. Soc.* **1989,** 136, 3206.

[S9] Y. J. Choi,N. W. Kim,K. W. Kim,K. K. Cho,G. B. Cho,H. J. Ahn,J. H. Ahn,K. S. Ryu, and H. B. Gu. *J. Alloy. Compd.* **2009,** 485, 462.